

# Optimal Allocation of Renewable Energy Resources to Improve Voltage Profile and Minimize Power Losses on the Most Critical Buses Prone to Voltage Instability

Okendo Edwin Otieno

Interdisciplinary Graduate School of Engineering Sciences, Kyushu University

Farzaneh Hooman

Interdisciplinary Graduate School of Engineering Sciences, Kyushu University

<https://doi.org/10.5109/7323244>

---

出版情報 : Proceedings of International Exchange and Innovation Conference on Engineering & Sciences (IEICES). 10, pp.68-73, 2024-10-17. International Exchange and Innovation Conference on Engineering & Sciences

バージョン :

権利関係 : Creative Commons Attribution-NonCommercial-NoDerivatives 4.0 International

## Optimal Allocation of Renewable Energy Resources to Improve Voltage Profile and Minimize Power Losses on the Most Critical Buses Prone to Voltage Instability

Okendo Edwin Otieno<sup>1</sup>, Farzaneh Hooman<sup>2</sup>

<sup>1</sup> Interdisciplinary Graduate School of Engineering Sciences, Kyushu University, Fukuoka 816-8580, Japan

<sup>2</sup> Interdisciplinary Graduate School of Engineering Sciences, Kyushu University, Fukuoka 816-8580, Japan

Corresponding author email:okendo.edwin.135@s.kyushu-u.ac.jp

**Abstract:** *The increased penetration of Renewable Energy Resources (RES), like solar and wind energy, into the grid, has addressed climate change challenges but also contributed to power system instability. This study proposes a methodology for the optimal allocation of solar and wind energy on the IEEE-33 bus radial distribution network to enhance the voltage profile and reduce active power losses. The methodology identifies the three most critical buses susceptible to voltage instability using the Fast Voltage Stability Index (FVSI) method. Various types and sizes of RES are allocated to these buses to evaluate their impact on voltage profile improvement and power loss reduction. Simulations are conducted using MATPOWER in MATLAB software. Results show that voltage profile enhancement and power loss reduction depend on the type, size, and location of RES, demonstrating the methodology's effectiveness compared to related studies.*

**Keywords:** *Renewable Energy Resources; Fast Voltage Stability Index; MATPOWER; MATLAB.*

### 1. INTRODUCTION

Conventional energy resources are major contributors to climate change due to their high carbon dioxide and greenhouse gas emissions [1]. Therefore, to combat climate change and achieve a net-zero emission society, there has been a global shift towards Renewable Energy Resources (RES), primarily wind and solar energy, which are clean, abundant, and sustainable [2], [3], [4]. However, RES face technical challenges due to their inappropriate integration into the existing electrical power distribution network, which may increase power losses and adverse effects on voltage profiles, leading to increased costs [5], [6]. Consequently, RES should be optimally allocated to ensure improved voltage stability, power quality, reliability, and minimized power losses, thereby enhancing the performance of the electrical grid. [7].

The literature review reveals that numerous authors have proposed various methods, including optimization and sensitivity-based approaches, to determine the optimal allocation of RES in electrical grid. Authors in [8], proposed Particle Swarm Optimization (PSO) and Differential Evolution algorithms for the optimal placement of different RES to reduce active power losses on some of the IEEE Radial Distribution Networks. The best results were obtained with PSO. Authors in [9] proposed a hybrid optimization method using PSO and Harris Hawks Optimization (HHO) method to reduce annual active power losses and enhance the voltage stability index through the optimal allocation of wind and solar energy on some of the selected IEEE radial distribution networks and the 94-bus system of the Portuguese radial distribution network. The authors in [10] proposed using Genetic Algorithm (GA) to optimally place various types of RES on the IEEE 33 and 69 bus radial distribution networks to minimize total active power losses. Authors in [11] proposed a Political Optimization algorithm to optimally allocate different types of distribution generations and shunt capacitors to

enhance voltage stability and minimize active power losses in 24 hours, on the IEEE-33 bus radial distribution network. Authors in [12] proposed using the PSO algorithm to optimally place a single type of RES with a maximum penetration of 41.15% to reduce active power losses on the IEEE-33 bus radial distribution network. The student Psychology-Based Optimization algorithm and HHO algorithm were used in [13] to optimally place RES with cost analysis. The method was successfully tested on the IEEE-33 and 69-radial distribution networks and the Brazilian -136 bus radial distribution network. Authors in [14] proposed optimal allocation and sizing of RES using PSO and voltage stability index (VSI) to enhance voltage profile and reduce active power losses. The proposed approach was tested and implemented on the IEEE-33 and IEEE-69 bus radial distribution network. The new VSI method and the GA is proposed in [15] to identify the most sensitive bus to voltage collapse to allocate RES on some of the selected IEEE radial distribution network.

From the literature survey, although various approaches for the optimal allocation of RES are based on the VSI, no research has specifically addressed the allocation of RES on the three most critical buses of the IEEE-33 bus radial distribution network identified by the Fast Voltage Stability Index (FVSI) method. Therefore, this research proposes the identification and allocation of RES on the three most critical buses of the distribution network using the FVSI method to enhance voltage profile and reduce active power losses. Additionally, this research considers the impact of the location of RES on voltage profile improvement and active power loss minimization by comparing the simulation results with those from the literature, an area previously unaddressed.

The first section of the paper serves as an introduction. The rest of the paper is divided into five sections. The mathematical formulation of VSI is presented in section two. Section three describes the study's methodology. Section four presents the results and discussion.

Section five provides the conclusion, and the final section, section six, lists some of the selected references for the study.

## 2. PROBLEM FORMULATION

The Fast Voltage Stability Index (FVSI) presented in [16] is used to calculate the VSI of each bus in the IEEE 33-bus radial distribution network. The FVSI values range from 0 to 1, where a higher index value close to 1 indicates lower voltage stability, while a lower index value close to 0 indicates higher voltage stability. The mathematical formulation of FVSI is presented in Equation 1.

$$F_{FVSI} = \frac{4Z_{ij}^2 Q_j}{V_i^2 X_{ij}} \quad (1)$$

Where;

$Z_{ij}$  represents the branch impedance linking bus  $i$  to bus  $j$

$Q_j$  is the receiving end reactive power flow

$V_i$  represents the sending end voltage magnitude

$X_{ij}$  represents the branch reactance linking bus  $i$  to bus  $j$

This study uses the IEEE 33-bus radial distribution network, operating at a nominal voltage of 12.66 kV. It comprises 32 branches and 33 buses, with the slack bus connected to bus 1. The remaining buses are connected to active loads totaling 3.72 MW and reactive loads totaling 2.3 MVar [17]. The details of the network are presented in [17], and the topology is shown in Figure 1. The network was modified in MATPOWER version 7.1 using MATLAB R2023b. The load flow method used in this study is the Newton-Raphson method, which is more efficient and less prone to divergence [18].

## 3. METHODOLOGY

The flow chart adopted to determine the optimal location of RES is as shown in Figure 2. This procedure assesses how different types and sizes of RES, based on their location within the distribution network, affect voltage profile improvement and active power loss reduction. Load flow studies using the Newton-Raphson method for the distribution network, modified in MATPOWER, are first conducted to determine the power flows. The power flow solutions are then used to calculate the VSI at different buses using Equation (1). The three most sensitive buses, with the highest voltage stability indices, are selected as the most critical buses. Next, the distribution network is modified in MATPOWER to allocate different RES types and sizes to the critical buses identified by the FVSI. Finally, load flow studies are conducted to determine the power flow solutions and assess the impact of different types of RES, their sizes, and locations on voltage profile and active power loss.

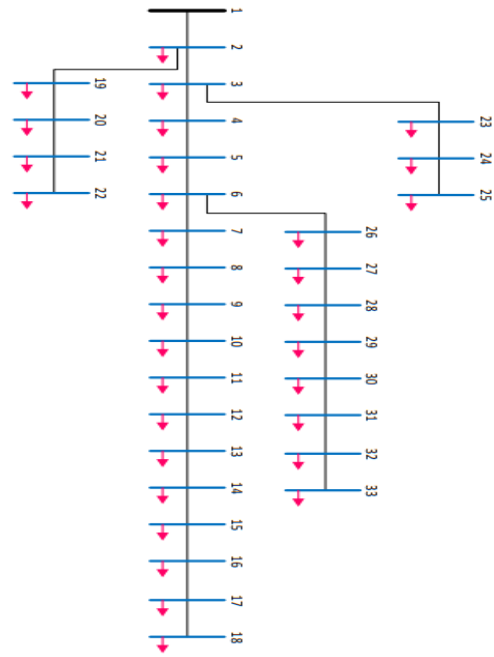


Fig. 1. The IEEE 33-Bus distribution network

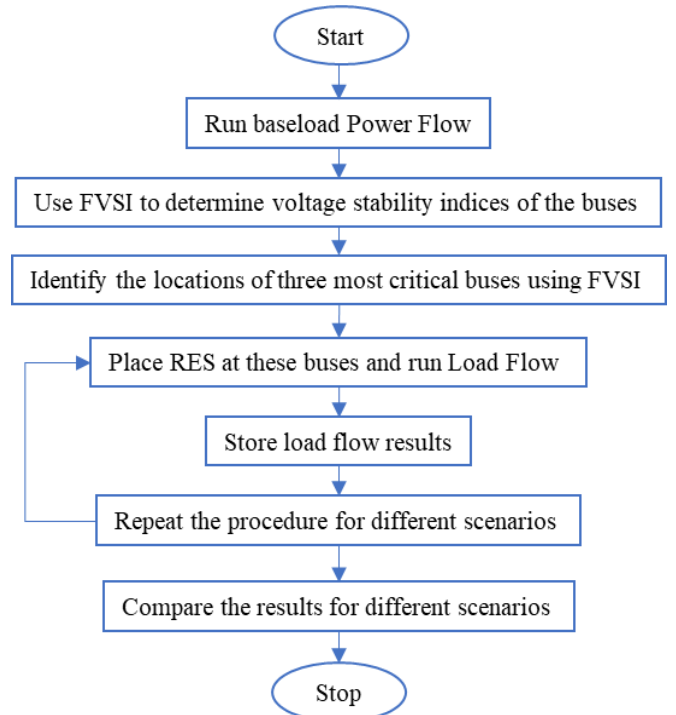


Fig. 2. Proposed flow chart for optimal location of RES.

## 4. RESULTS AND DISCUSSIONS

### 4.1 Baseload case: Scenario I

In Figure 3, the voltage profile simulation results are presented for the baseload case of the IEEE 33-bus distribution network, where no RES are incorporated. At baseload case, the total active power loss is 0.20 MW, while the total reactive power loss is 0.14 MVar. The active power losses at each bus are presented in Figure 5. Figure 4 presents the simulation results for the voltage stability indices at different buses of the distribution network. Bus number 6 is the most critical bus, with the highest FVSI value of 0.712, followed closely by bus 3, with an FVSI value of 0.695, and bus number 28, with an

FVSI value of 0.563. Buses 6, 3, and 28 were selected as the most critical buses for the optimal location of the RES.

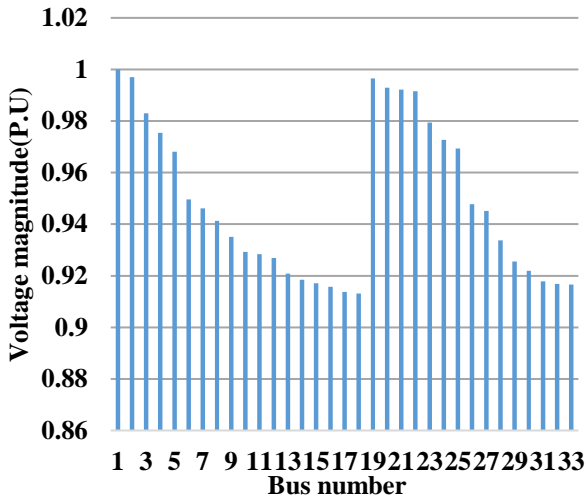


Fig. 3. IEEE 33-Bus distribution network voltage profile

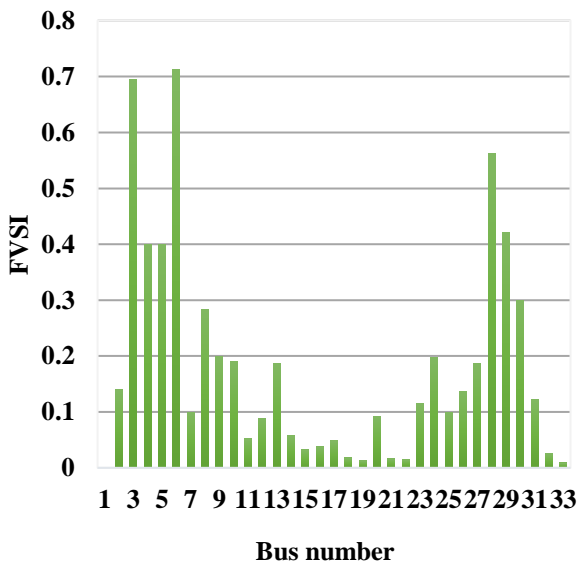


Fig. 4. IEEE 33-Bus distribution network FVSI

#### 4.2 Solar PV: Scenario II

Table 1 shows the different sizes of solar PV used in Scenario II, obtained from [19]. These solar PVs are arranged into three groups based on their sizes and locations.

In group one, only one solar PV, is allocated to bus number 6, which is identified as the most critical bus. The simulation results show the voltage profile, as depicted in Figure 5, with a total active power loss of 0.105 MW.

In group 2, two solar PV with different sizes are allocated to bus numbers 6 and 3. These buses have the highest FVSI values and are, hence, the most critical for voltage instability. The simulation results show the voltage profile, as depicted in Figure 5, with a total active power loss of 0.104 MW.

In group three, three solar PVs with different sizes are allocated to bus numbers 6, 3, and 28, which are the most critical buses for voltage instability.

The simulation results show the voltage profile, as depicted in Figure 5, with a total active power loss of 0.093 MW.

#### 4.3 Wind generator: Scenario III

From Table 2, six different sizes of wind generators are arranged into three distinct groups for use in Scenario III. In group one, only one wind generator, is allocated to bus number 6, which is identified as the most critical bus. The simulation results show the voltage profile, as depicted in Figure 7, with a total active power loss of 0.064 MW.

In group two, two wind generators with different sizes, are allocated to bus numbers 6 and 3, which have the highest FVSI values and are hence the most critical buses for voltage instability. The simulation results show the voltage profile, as depicted in Figure 7, with a total active power loss of 0.053 MW.

In group three, three wind generators with different sizes, are allocated to bus numbers 6, 3, and 28. The simulation results show the voltage profile, as depicted in Figure 7, with a total active power loss of 0.049 MW.

Table 1. Different sizes of solar PV, with their corresponding optimal location [19]

| Solar PV | Size   |      | Bus |
|----------|--------|------|-----|
| Group    | kW     | kVar |     |
| 1        | 2589.6 | ---  | 6   |
| 2        | 1898.7 | ---  | 6   |
|          | 649.9  | ---  | 3   |
| 3        | 1277.3 | ---  | 6   |
|          | 986.1  | ---  | 3   |
|          | 691.1  | ---  | 28  |

Table 2. Different sizes of wind generators with their corresponding optimal location [19]

| Wind  | Size   |        | Bus |
|-------|--------|--------|-----|
| Group | kW     | kVar   |     |
| 1     | 2558.2 | 1761.1 | 6   |
| 2     | 1171.2 | 188.1  | 6   |
|       | 1095.4 | 1667.0 | 3   |
| 3     | 1058.9 | 832.9  | 6   |
|       | 967.7  | 832.6  | 3   |
|       | 537.8  | 597.3  | 28  |

#### 4.4 Scenario II simulation results

From Figure 5, the voltage profile at the baseload scenario improves with an increase in the size of penetration of solar PV. Specifically, the voltage at bus 18, which initially had the lowest voltage of 0.90 per unit, improved to 0.98 per unit. Further improvements in the voltage profile at this bus are observed with the addition of 2 solar PV and 3 solar PV. The graph clearly shows that the voltage profile is enhanced with the increasing

penetration of various solar PV sizes, with larger sizes resulting in higher voltage improvements. Additionally, all bus voltages with solar PV fall within the acceptable voltage limits. Figure 6 presents graphs showing the total active power losses incurred before and after the inclusion of solar PV in baseload scenario I, where no solar PV is installed, with the total active power loss being 0.20 MW. However, with the inclusion of Solar PV, the losses are significantly reduced. Specifically, the power losses decrease to 0.105 MW with 1 solar PV, 0.104 MW with 2 solar PV, and 0.093 MW with 3 solar PV.

#### 4.5 Scenario III simulation results

Figure 7 shows that the voltage profile at the baseload case improves with an increase in the size of the penetration of the wind generator. Specifically, the voltage at bus 18, which initially had the lowest voltage of 0.90 per unit, improved to 0.98 per unit with the implementation of the wind generator. Further improvements in the voltage profile at this bus are observed with the addition of 2 wind generators and 3 wind generators. The graph shows that the voltage profile is enhanced with the increasing penetration of various sizes of wind generators, with larger sizes resulting in higher voltage improvements. Additionally, all bus voltages with wind generators fall within the acceptable voltage limits. Figure 8 presents graphs that illustrate the active power losses incurred in the buses of the distribution network before and after the inclusion of the wind generator. In the baseload scenario 1, where no wind generators are installed, the power losses amount to 0.20 MW. However, with the inclusion of wind generators, the losses are significantly reduced. Specifically, the power losses decrease to 0.064 MW with 1 wind generator, to 0.053 MW with 2 wind generators, and to 0.049 MW with 3 wind generators. This reduction in power losses with the inclusion of wind generators. From the graph, it is also evident that the power losses are significantly reduced by the size of the wind generator installed at the most critical buses identified by the FVSI voltage stability index.

#### 4.6 Comparison of Scenario II and Scenario III

Figures 5 and 7 show the impact of installing solar PV and wind generator, respectively, on the voltage profile of the IEEE-33 radial bus distribution network. From these figures, the voltage profile is improved, and all bus voltages remain within acceptable limits. This improvement is due to the higher active power compared to reactive power injected by the RES, which compensates for real power losses, thereby reducing overall power losses and enhancing the voltage profile. The impact of installing solar PV and wind generators on the active power losses of the distribution network is depicted in Figure 6 and 8, respectively. From these figures, it is evident that the installation of wind generator significantly reduces the active power losses compared to Solar PV. This difference is attributed to the reactive power injected by the wind generator.

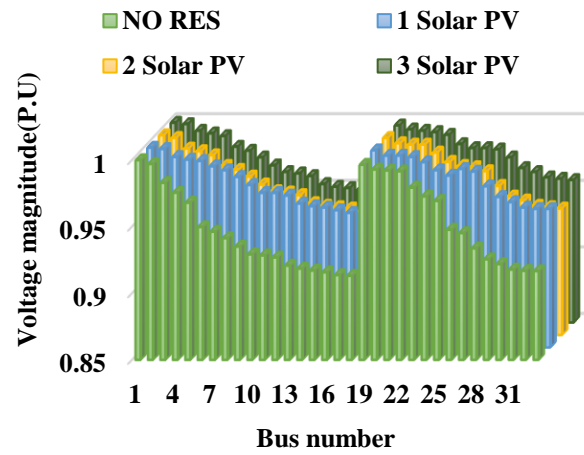


Fig. 5 Voltage profile of the IEEE-33 bus radial distribution network with different penetrations of solar PV.

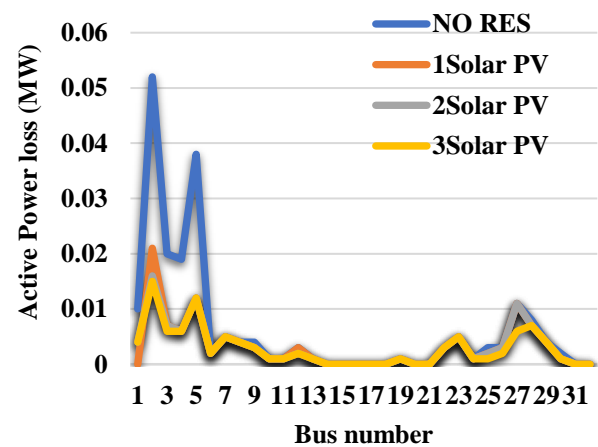


Fig.6. Power loss reduction using different sizes of solar PV.

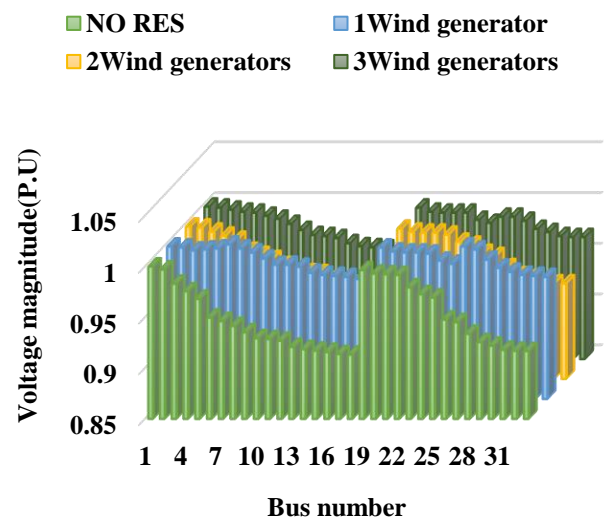


Fig.7. Voltage profile of the IEEE-33 bus radial distribution network with different penetration of wind generator.



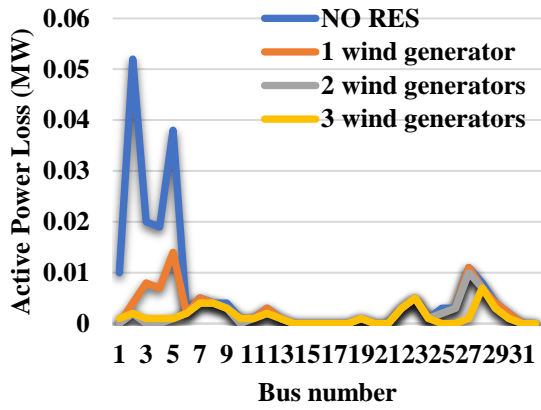


Fig.8. Power loss reduction using different sizes of wind generator.

#### 4.7 Validation

Tables 3 and 4 compare the different types, sizes, and locations of solar PV and wind generators, respectively, used in this study, along with the results of related studies recorded in [19].

Table 3. Comparison with other methods using solar PV

| Solar PV |        | Size |            | Bus number |            | % power loss reduction |  |
|----------|--------|------|------------|------------|------------|------------------------|--|
| Number   | kW     | kVar | (proposed) | [19]       | (proposed) | [19]                   |  |
| 1        | 2589.6 | ---  | 6          | 6          | 47.4       | 47.39                  |  |
| 2        | 1898.7 | ---  | 6          | 6          | 48.8       | 56.73                  |  |
|          | 649.9  | ---  | 3          | 14         |            |                        |  |
| 3        | 1277.3 | ---  | 6          | 29         | 54.2       | 64.88                  |  |
|          | 986.1  | ---  | 3          | 24         |            |                        |  |
|          | 691.1  | ---  | 28         | 14         |            |                        |  |

Table 4. Comparison with other methods using wind

The results of the proposed approach proved its

| Wind Generator |        | Size   |            | Bus number |            | % power loss reduction |  |
|----------------|--------|--------|------------|------------|------------|------------------------|--|
| Number         | kW     | kVar   | (proposed) | [19]       | (proposed) | [19]                   |  |
| 1              | 2558.2 | 1761.1 | 6          | 6          | 68         | 67.84                  |  |
| 2              | 1171.2 | 188.1  | 6          | 11         | 73.5       | 80.65                  |  |
|                | 1095.4 | 1667.0 | 3          | 30         |            |                        |  |
| 3              | 1058.9 | 832.9  | 6          | 24         | 75.86      | 90.70                  |  |
|                | 967.7  | 832.6  | 3          | 30         |            |                        |  |
|                | 537.8  | 597.3  | 28         | 13         |            |                        |  |

Table 3 demonstrates that the size and location of solar PV significantly impact the amount of active power loss reduction within the distribution network. The percentage of active power loss reduction increases with the size of the solar PV installed on the buses, both for the proposed approach and for the results recorded in [19]. Additionally, Table 3 shows that the solar PV location also contributes to power loss reduction. The optimal location selected by the PSO algorithm in [19] shows a

effectiveness in optimal allocation of RES compared to other related studies. The simulation results indicated that the voltage profile improvement and power losses reduction, are significantly influenced by several factors: the type of RES installed, their size, and their specific location within the distribution network. In summary, the findings emphasize the importance of careful planning and optimal allocation of RES to maximize their benefits,

which is crucial for achieving sustainable and efficient energy systems.

## 6. REFERENCES

- [1] M. Hidehito, M. Abdul, D. Manoj and S. Tomonobu, "Control strategy of PMSG based wind energy conversion system under strong wind conditions," *Energy for sustainable development*, no. 45, pp. 211-218, 2018.
- [2] N. ., Alphonse and F. Hooman, "Techno-economic analysis and dynamic power simulation of a hybrid solar-wind-battery-flywheel system for off-grid power supply in remote areas in Kenya," *Energy Conversion and Management: X*, no. 18, 2023.
- [3] M. Mehran and F. Hooman, "The role of local energy markets in low voltage networks: community-based approaches," in *Proceeding of International Exchange and Innovation Conference on Engineering & Sciences (IEICES)*, Fukuoka, 2023.
- [4] U. R. Nabeel and F. Hooman, "Techno-Economic Analysis of on Grid PV Power System for Vocational Training Institute in Baluchistan Pakistan to Reduce the Cost of Energy," in *Proceedings of the 8th International Exchange and Innovation Conference on Engineering & Sciences*, Fukuoka, 2022.
- [5] M. Badji, Z. Mohamed, C. Rachid and N. Hassan, "Optimal integration of renewable distributed generation using the whale optimization algorithm for techno-economic analysis," 2020.
- [6] M. V.V.S.N and A. Kumar, "Comparison of optimal DG allocation methods in radial distribution systems based on sensitivity approaches," *Electrical power and energy systems*, no. 53, pp. 450-467, 2013.
- [7] V. Vita, "Development of a decision-making algorithm for the optimum size and placement of distributed generation units in distribution networks," 2017.
- [8] H.Manafi, N.Ghadimi, M.Ojaroudi and P.Farhadi, "Optimal placement of distributed generations in radial distribution systems using various PSO and DE algorithms," *Electron.Elect.Eng*, vol. 19, no. 10, pp. 53-57, 2013.
- [9] E. M.R, E. M.Abd, Z.Ullah, S.Wang and S.W.Sharshir, "Optimal planning of renewable energy-integrated distribution system considering uncertainties," *IEEE Access*, vol. 7, pp. 164887-164907, 2019.
- [10] T.N.Shukla, S.P.Singh, V.Srinivasarao and K.B.Naik, "Optimal sizing of distributed generation placed on radial distribution systems," *Electr.Power Compon.Syst*, vol. 38, no. 3, pp. 260-274, 2010.
- [11] N.Dharavat, S. Sudabattula and S.Velamuri, "Optimal allocation of multiple distributed generators and shunt capacitors in a distribution system using political optimization algorithm," *Int J. Renew. Energy Res*, vol. 11, no. 4, pp. 1478-1488, 2021.
- [12] N.Hantash, T.Khatib and M.khammash, "An improved PSO algorithm for optimal allocation of distributed generation units in a radial power systems," *Appl. Comput. Intell. Soft Comput.*, pp. 1-8, 2020.
- [13] K.Babu and V.Mukherjee, "Optimal siting and sizing of distributed generation in radial distribution system using a novel student psychology-based optimization algorithm," *Neural Comput. Appl*, vol. 33, pp. 15639-15667, 2021.
- [14] P. Anshuman, T. Tripta and S. Gupta, "Voltage stability index based optimal sizing and placement of DG," *IEEE. Conf*, 2020.
- [15] S. Hadavi, B. Zaker, H. Karami, A. A. A. Khodadoost and G. B. Gharehpetian, "Optimal Placement and Sizing of DGs Considering Static Voltage Stability," *Electric. Pow. Conf.*, 2017.
- [16] S. S. Hossam and V. Istavan, "Voltage stability indices–A comparison and a review," *Computers and Electrical Engineering*, vol. 98, 2022.
- [17] M.Purlu and B.E.Turkay, "Optimal allocation of renewable distributed generations using heuristic methods to minimize annual energy losses and voltage deviation index," *IEEE Power and energy society section*, 2022.
- [18] S. HADI, *Power system analysis*, London: McGraw-Hill, 1999.
- [19] D.B.Prakash and C.Lakshminarayana, "Multiple DG placement in distribution system for power loss reduction using PSO algorithm," *Procedia Technology*, no. 25, pp. 785-792, 2016.